Reactive blue dye detects male reproductive toxicity

Satoshi Yokota[1]*, Tomohiko Wakayama[2], Hidenobu Miyaso[3], Kousuke Suga[1], Masakatsu Fujinoki[4], Satoru Kaneko[5] and Satoshi Kitajima[1]

[1] Division of Cellular & Molecular Toxicology, Center for Biological Safety & Research, National Institute of Health Sciences, Kawasaki, Kanagawa, Japan, [2]Department of Histology, Graduate School of Medical Sciences, Kumamoto University, Honjo, Kumamoto, Japan, [3]Department of Anatomy, Faculty of Medicine, School of Medicine, International University of Health and Welfare, Narita, Chiba, Japan, [4]Research Lab. of Laboratory Animals, Research Center for Laboratory Animals, Comprehensive Research Facilities for Advanced Medical Science, School of Medicine, Dokkyo Medical University, Tochigi, Japan, and [5]Department of Obstetrics and Gynecology, Ichikawa General Hospital, Tokyo Dental College, Ichikawa, Chiba, Japan.

*Correspondence should be addressed to Satoshi Yokota, Division of Cellular & Molecular Toxicology, Center for Biological Safety & Research, National Institute of Health Sciences, 3-25-26 Tono-machi, Kawasaki-ku, Kawasaki, Kanagawa 210-9501, Japan; e-mail: s-yokota@nihs.go.jp

Keywords: reactive blue 2; protamine; male reproductive toxicity

Abstract

Background: Reactive blue 2 (RB2) dye specifically binds to the nuclei of spermatozoa under weakly alkaline conditions, thus providing a new method to assess human sperm quality. However, this technique has not yet been applied to other mammalian species, such as well-established rodent models, which could enable evaluation of the testicular toxicity of drug candidates in non-clinical studies.

Objectives: We sought to examine the usefulness of the novel RB2 staining technique for evaluating mouse testicular and epididymal sperm toxicity using a common busulfan-induced infertility mouse model.

Materials and methods: Busulfan (40 mg/kg) was intraperitoneally administered to C57BL/6J male mice. Twenty-eight days later, the testes and epididymis were collected and stained with RB2 at pH 10. RB2 was mixed with protamines extracted from the spermatozoa or intracellular protein components from somatic cells (HeLa cells) without protamines for *in vitro* evaluation on a non-coated slide glass.

Results: RB2-positive cells were observed in elongating and elongated spermatids at all stages except for stages IX–XI of the seminiferous epithelium, following peanut agglutinin (PNA) lectin

histochemistry. The percentage of RB2-positive germ cells in the seminiferous tubules significantly decreased after busulfan administration. There were no RB2-positive spermatozoa in the caput epididymis of busulfan-treated mice. Aggregates were observed in the mixture of RB2 dye (pH 10) with protamines but not in the mixture of intracellular protein components without protamines. This specificity was lost at neutral pH.

Discussion and Conclusion: Identification of the stage of mouse seminiferous tubules using PNA lectin histochemistry revealed that RB2 specifically stains stage 12–16 spermatids, indicating specific binding to protamine expressed at these stages. This novel RB2 staining technique could be helpful for the rapid visualization of protamination as a biomarker of male reproductive toxicity.

Introduction

The International Council for Harmonisation of Technical Requirements for Pharmaceuticals for Human Use guidelines require histopathological evaluation of the effects of a candidate drug using hematoxylin-eosin (HE) staining in non-clinical animal studies, including general toxicity studies as well as male reproductive toxicity studies.[1] Specifically, testicular toxicity must be evaluated prior to the first clinical trial in humans. If pharmaceutical candidates are shown to have potential testicular toxicity, non-clinical animal testing does not proceed. Although there are no specific recommendations in regulatory guidelines for general toxicity studies using animals regarding the evaluation of male reproductive toxicity, non-clinical testicular toxicity testing could be preferable to detect similar changes that may occur in clinical trials. However, the results of non-clinical animal testing do not necessarily match the effects in humans.[2,3] Furthermore, identification and interpretation of chemically induced changes in testis histology require fundamental knowledge of spermatogenesis; however, there is currently no staining technique available to specifically identify male germ cell development in complicated histology. Thus, the development of a novel method to specifically stain spermatogenic cells is needed to support the interpretation of the results of histopathological analysis using HE staining.

43 During the late haploid phase of spermatogenesis (spermiogenesis), mammalian
44 spermatozoa undergo protamination in which approximately 90% of the histones that package
45 DNA in early spermatids are removed from the DNA and are replaced by transition nuclear
46 proteins and finally by protamines (PRMs).[4] PRMs possess more domains rich in arginine (Arg),
47 a basic amino acid, than histones and transition nuclear proteins to promote sperm head
48 condensation and DNA stabilization by binding to the phosphoric group in DNA.[5] The importance
49 of PRMs in sperm chromatin condensation and the influence of protein expression on sperm
50 function have been shown in both mouse and human studies.[6-9] In most mammals, the sperm
51 chromatin is packaged by a single PRM, whereas primates and most rodents, as well as subset of
52 other placental mammals, express two PRMs: protamine 1 (PRM1) and protamine 2 (PRM2).
53 Alterations in the content of sperm PRMs induce negative effects on sperm concentration, motility,
54 and sperm head morphology in men.[8] Haploinsufficiency of PRMs in mice results in sperm
55 morphological abnormalities, DNA damage, and decreases in sperm motility.[10] In particular,
56 PRM2 deficiency has a negative impact on chromatin packaging and sperm head morphology.[7]
57 Incorrect condensation of sperm chromatin leads to head abnormalities such as larger heads.[11]
58 These findings suggest that PRM levels could serve as a biomarker of male infertility.[6]

59 A previous study showed that reactive blue 2 (RB2) dye specifically bound to the nucleus
60 of spermatozoa under weakly alkaline conditions (pH 10), offering a new method to assess human
61 sperm quality.[12] At this weakly basic pH, three sulfate residues in the RB2 molecule may, in
62 principle, bind electrostatically to the guanidyl groups in Arg, enabling specific staining of PRMs
63 in human spermatozoa.[12] Considering the chemical structure of RB2, we hypothesized that RB2
64 binding is a specific dye for PRMs in male haploid germ cells under weakly alkaline conditions.
65 However, testicular histological analysis is needed for invasive procedures such as biopsy;
66 therefore, it is difficult to confirm the specificity of RB2 to human testicular germ cells. Therefore,
67 it would be useful to apply RB2 staining in non-clinical studies for evaluating male reproductive
68 toxicity in rodent models; however, this technique has not yet been attempted in mammalian
69 species other than humans.

70 Therefore, the aim of the present study was to examine whether the germ cell specificity
71 of RB2 found in humans is consistent in experimental mammalian models such as mice, which
72 would enable research on drug toxicity in the context of complicated testicular histology.
73 Specifically, we examined whether PRMs could be visualized by RB2 using an *in vitro* experiment
74 to examine the usefulness of this novel staining technique for evaluating mouse testicular and

75 epididymal sperm toxicity using a standard mouse model of infertility established by the
76 administration of busulfan.[13-16]
77

78 Materials and Methods

79 Animals

80 Twelve C57BL/6J male mice (CLEA Japan, Tokyo, Japan) aged 5 weeks were maintained
81 under standard laboratory conditions. The mice were housed individually in ventilated cage
82 systems (Lab Product Inc., Seaford, DE, USA) at 23 ± 2°C under a 12-h light/dark cycle (lights on
83 from 8:00 to 20:00), with food and water provided *ad libitum*. Body weight was measured once a
84 week (three mice per cage). This study followed the guidelines established by the Ethical
85 Committee for Animal Experiments of the National Institutes of Health Sciences (NIHS). The
86 animal facility was approved by the Health Science Center for the Accreditation of Laboratory
87 Animal Care in Japan. All experimental protocols in the study were reviewed and approved by the
88 Committee for Proper Experimental Animal Use and Welfare, a peer-review panel established at
89 the NIHS, under experimental approval no. 816.
90

91 **Experimental design**

92 After 1-week habituation, the 12 mice were randomly divided into two groups: vehicle
93 control group (n = 6) and busulfan-treated group (n = 6). The vehicle control group received two
94 intraperitoneal (i.p.) injections of vehicle containing 10% dimethyl sulfoxide (DMSO; 031-24051;
95 CultureSure®DMSO; FUJIFILM Wako Pure Chemical Industries, Ltd., Osaka, Japan) in saline
96 (Otsuka Pharmaceutical Co.; Tokyo, Japan) with a 3-h interval between injections. Busulfan (B-
97 2635; Sigma-Aldrich, St. Louis, MO, USA) was dissolved in DMSO at a concentration of 10
98 mg/mL and then gradually added to a nine-times volume of saline (final concentration: 1 mg/mL).
99 Similar to the vehicle control group, the busulfan-treated group also received two i.p. injections
100 (20 mL/kg per injection) of busulfan at a total dose of 40 mg/kg body weight, as previously
101 described.[13, 17] After 28 days, the reproductive organs of the male mice were collected under
102 isoflurane anesthesia. All efforts were made to minimize animal suffering. Each mouse was
103 weighed, blood was collected from the inferior vena cava, and the testes and epididymis were
104 removed. Dissected tissues were fixed for histopathological analysis as described below.

105

106 **Isolation of spermatozoa from the caput or cauda epididymis and RB2 staining**

107 For isolation of spermatozoa, the caput or cauda epididymis from each animal was cut using
108 a surgical blade and then minced using small scissors in 10 mM HEPES-buffered TYH culture
109 medium (119 mM NaCl, 4.8 mM KCl, 1.7 mM $CaCl_2$, 1.2 mM KH_2PO_4, 1.2 mM $MgSO_4$, 25 mM
110 $NaHCO_3$, 5.6 mM glucose, 1.0 mM sodium pyruvate, and 4 mg/mL bovine serum albumin; pH
111 7.4). Briefly, an aliquot of the caput- or cauda-derived sperm suspension was smeared on a glass
112 slide using a centrifugal auto-smear (Cyto-Tek; Sakura, Tokyo, Japan). The spermatozoa were then
113 fixed with methanol for 5 min and stained with 0.1% RB2 (catalog no. 12236-82-7; RB2; R115;
114 Sigma-Aldrich) in 100 mM carbonate-bicarbonate buffer (pH 10) for 30 min. The excess dye was
115 washed out with carbonate-bicarbonate buffer. The slides were mounted using ProLong Diamond
116 Antifade Mountant (P36961; Thermo Fisher Scientific, Kyoto, Japan) prior to microscopic
117 examination. We observed 200 spermatozoa per mouse (n = 6 per group) using a microscope
118 (BX51; Olympus Co., Tokyo, Japan) equipped with cellSens imaging software (Olympus Co.,
119 Tokyo, Japan).
120

121 **RB2 staining of spermatids in the testes and of spermatozoa in the epididymis**

122 For histopathological analysis, the testes and epididymis were removed and immersed in a
123 freshly prepared 4% paraformaldehyde phosphate buffer fixative (161-20141; FUJIFILM Wako
124 Pure Chemical Industries, Ltd.) for 48 h. Following fixation, the testes and epididymis were
125 processed using a graded alcohol series, cleared in xylene, and embedded in paraffin. Sections (4-
126 μm thick) were prepared, deparaffinized, and stained with HE using our routine method for overall
127 morphological evaluation. Two serial testis sections were prepared: one was used for visualization
128 of male germ cells expressing protamine according to RB2 staining, and the other was applied for
129 staging of the mouse seminiferous epithelium cycle using peanut agglutinin (PNA) lectin
130 histochemistry, as previously described.[18, 19] For the former analysis, the testicular and epididymal
131 cross-sections were stained with 0.1% RB2 in 100 mM carbonate-bicarbonate buffer (pH 10) for
132 30 min, and the excess dye was then washed out with the carbonate-bicarbonate buffer. For the
133 latter, the sections were immersed in 20 mM Tris-HCl buffer (pH 9) and heated at 90°C for 30 min
134 for antigen retrieval. After cooling to room temperature, the sections were washed in phosphate-
135 buffered saline, incubated with Alexa Fluor 488-conjugated lectin PNA antibody (L21409, 1:1000;
136 Molecular Probes, Eugene, OR, USA) for 30 min at room temperature to visualize the acrosomes,
137 and then counterstained with Hoechst 33258 (Sigma-Aldrich). Each stage of spermatogenesis was

138 determined to simplify the identification of the cell population, as previously reported.[18, 19] Briefly,
139 testis sections from the control mice were observed to determine the staging of the seminiferous
140 epithelium cycle. The 12 stages (I–XII) of spermatogenesis in mice were then determined using
141 the combination of PNA lectin histochemistry for the acrosomes of spermatids and Hoechst
142 staining for chromatin in the nuclei, according to the established criteria of stages based on the
143 position, size, and shape of acrosomes.

144 The slides were mounted using ProLong Diamond Antifade Mountant (P36961; Thermo
145 Fisher Scientific) prior to microscopic examination. To quantify the proportion of RB2-positive
146 germ cells in the seminiferous tubules, 200 seminiferous tubule sections were observed in two
147 tissue sections obtained from two discrete portions of a testis from a single mouse. We evaluated
148 the two tissue sections per mouse (n = 6 per group) using the BX51 microscope equipped with
149 cellSens imaging software.

150

151 **Analysis of motility of spermatozoa**

152 Spermatozoa were collected according to our previously reported method with minor
153 modifications.[19, 20] Briefly, the cauda epididymis was dissected, and the connective tissue, fat pad,

154 muscles, and vas deferens were removed. For sampling of spermatozoa, the cauda epididymis from
155 each animal was cut using a surgical blade and then minced using small scissors in 10 mM HEPES-
156 buffered TYH culture medium, as described above. The suspensions of spermatozoa were left to
157 disperse and swim up for 15 min on a warming tray at 37°C. The suspension was then filtered
158 through a 40-μm nylon filter (PP-40N; Kyoshin Rikoh, Tokyo, Japan) to remove any undigested
159 tissue fragments and cauda spermatozoa were collected to evaluate motility. The motile
160 spermatozoa were incubated for 2 h at 37 °C to allow for hyperactivation.

161 The percentage of motile or hyperactivated spermatozoa was measured on a 37°C heated
162 stage of a constant-temperature unit (MP-10; Kitazato Supply Co., Shizuoka, Japan), according to
163 a previously described method.[20] Sperm motility was recorded using a phase-contrast microscope
164 (CX43; Olympus, Tokyo, Japan) with Moticam 1080 (Shimadzu Rika Co., Tokyo, Japan). Using
165 a 10× phase-contrast objective, each field was recorded for 30 s, and the numbers of total
166 spermatozoa and motile and/or hyperactivated spermatozoa were manually counted in three
167 random fields for each sample. The analyses were performed in a blinded manner. Motile
168 spermatozoa that exhibited asymmetric and whiplash flagellar movements and a circular and/or
169 octagonal swimming locus were defined as hyperactivated.[20, 21] The percentage of motile

170 spermatozoa was calculated as the number of forward motile and sub-motile spermatozoa or
171 hyperactivated spermatozoa/total number of spermatozoa × 100 (%).
172
173 ***In vitro* experiment of RB2 binding**
174 RB2 dye in 100 mM carbonate-bicarbonate buffer (pH 10) was mixed with human spermatozoa
175 PRM (Briar Patch Biosciences, CA, USA) or mouse synthetic PRM1 or PRM2 (Briar Patch
176 Biosciences) on non-coated glass slides. After the reaction, the glass slides were mounted using a
177 mountant and observed under a microscope. As a negative control, bovine serum albumin (BSA;
178 23209; Pierce™ BSA standard ampules, 2 mg/mL; ThermoFisher Scientific, Waltham, MA, USA)
179 and an extracted intracellular protein from HeLa cells were mixed with RB2 dye (pH 10). HeLa
180 cells were cultured in Dulbecco's modified Eagle's medium (D5030, Sigma-Aldrich)
181 supplemented with 10% fetal bovine serum (10099, Thermo Fisher Scientific) and 100 μg/mL
182 kanamycin (420311, Sigma-Aldrich). The cells were lysed with sodium dodecyl sulfate (SDS)
183 lysis buffer (100 mM Tris-HCl at pH 8, 10% glycerol, and 1% SDS) to extract the intracellular
184 proteins.
185

186 **Statistical analysis**

187 Data are presented as mean ± standard deviation (GraphPad Prism version 9, GraphPad
188 Software Inc., San Diego, CA, USA). Welch's t-test was used to detect significant differences
189 between the control and busulfan-treated groups (GraphPad Prism version 9). Statistical
190 significance was assessed at $P < 0.05$.

191

192 ## Results

193 **Body and organ weights**

194 There were no significant differences in body weights of the control and busulfan-treated mice
195 (control; 25.3 ± 0.7 g, busulfan-treated; 24.9 ± 0.4 g). The absolute weights of the testes (left:
196 control = 104.6 ± 3.1 mg, busulfan-treated = 32.6 ± 2.7 mg, $P < 0.001$; right: control = 108.7 ± 7.8
197 mg; busulfan-treated = 31.5 ± 3.9 mg, $P < 0.001$) and the epididymis (left: control = 36.4 ± 3.3 mg,
198 busulfan-treated = 25.3 ± 2.0 mg, $P < 0.001$; right: control = 36.6 ± 3.2 mg, busulfan-treated =
199 25.6 ± 2.2 mg, $P < 0.001$) were significantly lower in the busulfan-treated mice than in the control
200 mice. In particular, the caput epididymis of busulfan-treated mice was grossly much smaller than
201 that of the control mice (**Data not shown**).

202

203 **RB2 specifically stains male haploid germ cells expressing PRMs**

204 Based on the shape of the acrosomes of the round and elongating spermatids (steps 1–12), the
205 corresponding staging of the mouse seminiferous epithelium cycle was determined (stages I–XII).
206 After identification of the germ cell population by staging of the mouse seminiferous epithelium
207 cycle (**Figure 1A, C, E, G, I, K, M, O, Q, S, U, W**), using the adjacent testis sections from the
208 control mice, RB2-positive cells were observed in steps 12 to 16 of elongating and elongated
209 spermatids in stages XII and I to VIII, but not in stages IX to XI of the seminiferous epithelium
210 cycle (**Figure 1B, D, F, H, J, L, N, P, R, T, V, X**).

211 Quantitative histological analysis showed that busulfan-treated mice had approximately half of
212 the seminiferous epithelium tubules than those in the control, with loss of step 12 to 16 elongating
213 and elongated spermatids (**Figure 2A–G**).

214

215 **RB2 staining to evaluate epididymal sperm toxicity**

216 The percentage of motile spermatozoa in busulfan-treated mice was significantly lower than that
217 in control mice ($P < 0.01$) (**Figure 3A**). The percentage of hyperactivated spermatozoa in busulfan-

218 treated mice also showed a significant decrease compared with that in the control group ($P < 0.05$)
219 (**Figure 3B**). Swim-up spermatozoa collected from the cauda epididymis of both control (**Figure**
220 **3C**) and busulfan-treated (**Figure 3D**) mice were stained with RB2. Spermatozoa collected from
221 the caput epididymis in control mice were also stained with RB2 (**Figure 3E**), whereas those of
222 busulfan-treated mice showed no positive staining (**Figure 3F**).
223 RB2-positive germ cells were detected in the caput epididymis of the control mice (**Figure**
224 **4A, C, E, G**), but not in the caput epididymis of busulfan-treated mice (**Figure 4B, D, F**), matching
225 the observations of the spermatozoa collected from the caput epididymis (**Figure 3E**).
226
227 **pH-dependence of RB2 specificity for PRMs**
228 Aggregates were observed in the mixture of RB2 dye (pH 10) with both human spermatozoa
229 PRMs and mouse synthetic PRMs (**Figure 5A–F**) but were not detected in the mixture with BSA
230 and the extracted intracellular proteins from HeLa cells (**Figure 5G–I**). In addition, this PRM
231 specificity of RB2 was lost at neutral pH in which both PRMs and histones of the somatic cells
232 were positively stained (data not shown).
233

234 **Discussion**

235 Histopathology of the testes is the best non-clinical endpoint for the evaluation of
236 testicular toxicity. However, identification and interpretation of chemically induced side effects on
237 testis histology require fundamental expertise in spermatogenesis. If a drug candidate compound
238 has side effects on male germ cell development, further efforts toward drug evaluation should be
239 avoided. However, the results of non-clinical animal testing may not necessarily align with the
240 effects found in humans.[2, 3] Ideally, it is desirable to have an evaluation system that can easily
241 determine testicular toxicity with as much accuracy as possible in non-clinical toxicological
242 studies of drug development. However, there is currently no available staining technique to identify
243 male germ cell development, specifically in cases of complicated histology.

244 Kaneko et al.[12] demonstrated that RB2 dye at pH 10 specifically stained the nucleus of
245 human spermatozoa without staining other cellular components of the human seminal fluid,
246 providing a new method to evaluate sperm quality. The present study further demonstrates that this
247 RB2 staining technique is also applicable to other mammalian species such as well-established
248 rodent models used for evaluation of the testicular toxicity of drug candidates in pre-clinical
249 studies, providing a novel staining technique for visualizing the nuclei of male mouse haploid germ

250 cells. This demonstration that both human and rodent spermatogenic cells can be visualized by
251 RB2 staining may be useful for extrapolation of the effects of pharmaceuticals on the testes and
252 epididymis of rodents to humans in a non-clinical toxicity test under conditions of limited time
253 and resources.

254 In mice, the 12 stages (stages I–XII) of spermatogenesis were determined using the
255 combination of PNA lectin histochemistry for the acrosomes of spermatids and Hoechst staining
256 for the chromatin in the nuclei, according to the established criteria of stages based on the position,
257 size, and shape of acrosomes, which is a common method to clearly identify step 1–16
258 spermatids.[18, 19] With this approach, we found that RB2 staining could only visualize steps 12–16
259 haploid elongating and elongated spermatids, but not spermatogonia, spermatocyte, and steps 1–
260 11 spermatids at pH 10; these findings match those for human spermatozoa.[12] Primates and most
261 rodents, as well as a subset of other placental mammals, express two PRMs: PRM1 and PRM2.[6]
262 Both genes are transcribed in round spermatids (steps 7–9 in mice)[22, 23], and the mRNA is then
263 stored in the form of cytoplasmic ribonucleoprotein particles until their translation in elongating
264 and elongated spermatids (steps 12–16).[24, 25] Following transcript storage, mouse *Prm1* mRNA
265 seems to be translated earlier (stage 12) than *Prm2* mRNA (stage 14, 15).[26] Therefore, our results

266 suggest that RB2 stain specifically binds to PRMs expressed in the step 12–16 haploid spermatids
267 in mouse seminiferous tubules.[24-26]

268 We further detected aggregates in the mixture of RB2 dye (pH 10) with human sperm PRM-
269 or mouse synthetic PRM reference standards, but not with BSA standard or intracellular proteins
270 without PRMs extracted from the lysis of somatic cells (HeLa cells). These results suggest that a
271 certain molecular component of PRMs can chemically interact with a component of RB2.
272 Coomassie brilliant blue (CBB) staining is a widely used method for the routine visualization of
273 various proteins such as BSA, which binds via ionic bonds and van der Waals forces. However,
274 CBB staining is not specific for a certain protein, requiring an additional protein separation step
275 for identification, such as polyacrylamide gel electrophoresis.[27] The present study thus highlights
276 the use of RB2 dye as a novel staining technique capable of the rapid and specific visualization of
277 PRMs without protein separation, which could offer breakthroughs in the field of reproductive
278 toxicology and andrology.

279 We further explored the mechanism by which RB2 dye stains PRMs. We hypothesized that
280 the unique binding specificity of RB2 with PRMs indicates an electrostatic ionic interaction.
281 Lysine (Lys) and Arg are two positively charged amino acids in proteins that have high aqueous

282 dissociation constants (~10.5 for lysine[28] and ~12.5 for Arg[29]), indicating a strong propensity to
283 carry a positive charge at neutral pH. In contrast, at pH > 10, Arg is a positively charged amino
284 acids, whereas Lys is a neutral residue.[28, 29] Therefore, the negative charge of the three sulfate
285 residues in RB2 could ionically combine with the guanidyl group in Arg at pH 10, but not with the
286 neutral chemical components of lysine. The present study demonstrated that RB2 specifically
287 stained step 12–16 spermatids, in which the majority of PRMs are translated, at pH 10, as
288 previously reported.[24-26], whereas the specificity of RB2 staining was lost at neutral pH when both
289 Lys and Arg are positively charged. This pH-dependent specificity could be due to differences in
290 the Arg content among the basic proteins, histones, transition proteins, and PRMs. PRMs are
291 typically short basic proteins with a high number of positively charged Arg-rich residues, allowing
292 the formation of a highly condensed complex with the paternal genomic DNA, which has a strong
293 negative charge.[30-33] The higher Arg content thus allows PRMs to form more stable complexes
294 with DNA than other basic proteins such as histones and transition proteins.[4] Lys and Arg account
295 for approximately 20–30% of the amino acids in histones, whereas Arg accounts for 70% of the
296 amino acids in PRMs.[4] Thus, the higher content of Arg in the PRMs of the step 12–16 spermatids

297 could explain the specificity of the novel RB2 staining technique under weakly alkaline conditions
298 (pH 10).

299 Finally, with respect to the technical application of this method for male reproductive
300 toxicity evaluation, we demonstrated that the percentage of RB2-positive spermatids in the
301 seminiferous tubules of mice was decreased following busulfan administration. In addition, no
302 RB2-positive spermatozoa were detected in the caput epididymis of busulfan-treated mice,
303 whereas spermatozoa of the cauda epididymis were stained with RB2 in both control and busulfan-
304 treated mice. These results suggest that busulfan administration during spermiogenesis and sperm
305 maturation decreases the abundance of PRMs to cause male infertility. Indeed, busulfan treatment
306 significantly decreased the percentage of motile or hyperactivated spermatozoa, as a common
307 index of male fertility. These results suggest that the RB2 staining technique can offer a rapid
308 assessment of the male reproductive toxicity of a drug, such as spermatogenic dysfunction and/or
309 impairment of sperm maturation, with simple visualization of the protamination of male haploid
310 germ cells, providing useful and supportive data to complement the results of conventional HE
311 staining.

312 The proposed method offers a more convenient and rapid tool for the visualization of PRMs
313 compared with immunohistochemical analysis using anti-PRM antibodies, which will be useful
314 not only for the field of reproductive toxicology but also in general research in the fields of
315 reproductive medicine and andrology to improve the diagnosis of infertility in both humans and
316 rodents. Altered levels of PRMs may result in increased susceptibility to injury of the spermatozoa
317 DNA, causing infertility or poor outcomes in assisted reproduction.[34] In general, mammalian
318 reproduction relies on successful transport of the paternal genome to the oocyte via motile
319 spermatozoa, and the formation of functional spermatozoa requires a specific and well-
320 orchestrated differentiation process in the testes.[35] PRMs have been suggested to be important for
321 remodeling of the chromatin complex following the elongation and condensation of the
322 spermatogenic cell nucleus into a hydrodynamic shape.[34, 36] Paternal chromatin is completely
323 remodeled from nucleo-histones (nucleosomes) to nucleo-protamines during spermiogenesis to
324 prepare for fertilization.[6, 34] In clinical studies, PRM deficiency was found to be related to the
325 exacerbation of sperm quality and to cause DNA fragmentation.[37] Thus, application of
326 spermatozoa with abnormalities in PRM abundance during assisted reproductive technology raises
327 serious concerns for the developing embryo.[38] Therefore, altered PRM abundance in spermatozoa

328 could serve as an important biomarker of male infertility. In this regard, use of RB2 as a novel and
329 specific staining technique of PRMs could enable the rapid evaluation of protamination during
330 spermiogenesis as supportive data for histopathological analysis in assisted reproduction.

331 Another major finding of the present study was that RB2 staining did not detect any
332 spermatozoa in the caput epididymis within 28 days after the administration of busulfan to mice
333 at 40 mg/kg body weight. Spermatogenesis is a complex process in which many spermatozoa are
334 produced from a relatively small pool of spermatogonial stem cells, which occurs during the entire
335 reproductive life of males.[35] To the best of our knowledge, most studies on busulfan have focused
336 largely on the testicular toxicity. As an alkylating agent, busulfan causes DNA damage by cross-
337 linking DNA, and was reported to specifically kill A1 spermatogonia (a type of spermatogonial
338 stem cell) as a side effect.[39] In mice, busulfan administered at 40 mg/kg body weight caused
339 complete depletion up to the pachytene spermatocytes in stage VIII within 12 days.[40] Since the
340 proliferation and differentiation of A1 spermatogonia into elongated spermatids takes
341 approximately 34.4 days in the testes[35], the spermatozoa in the caput epididymis were not
342 considered to be triggered by damage to the A1 spermatogonia within 28 days after busulfan
343 administration. In general, epididymal sperm toxicity evaluation may be more challenging than

344 the evaluation of testicular toxicity. The epididymis is a single, highly convoluted duct lined by a
345 complex pseudostratified epithelium consisting of multiple cell types, including principal cells,
346 basal cells, clear cells, apical cells, and halo cells.[41] The number and appearance of individual cell
347 types also vary between the segments of the epididymis (i.e., initial segment, caput, corpus, and
348 cauda). The present study demonstrated that RB2 is a specific dye for staining the spermatozoa
349 and could therefore increase the throughput of epididymal toxicity evaluation.

350 In conclusion, we have demonstrated a novel methodology for visualizing male haploid
351 germ cells using RB2 dye, which provides an important basis for evaluating the effects of
352 pharmaceuticals such as anticancer drugs on testicular and epididymal toxicity. However, this
353 study had some limitations. The data obtained were insufficient for time-course evaluation.
354 Spermatogenesis is a continuous, cyclical, and synchronized process that occurs in the epithelium
355 of the seminiferous tubules of the testes, spanning approximately 34.4 days in mice and 74 days
356 in humans.[35] In addition, sperm maturation requires approximately 10 days in both mice and
357 humans.[35] Chemicals may influence the testes and epididymis at any time point in these cycles.
358 Therefore, it is difficult to predict precisely when and where testicular and epididymal toxicity
359 may occur, which should not be evaluated at only one time point but rather over several time points

360 to further assess the potential recovery from drug toxicity, which is particularly important for
361 anticancer drugs. Thus, further investigations are needed to evaluate the time-course changes in
362 PRMs abundance in histological testes specimens and in the spermatozoa using the RB2 staining
363 technique.
364

365 Acknowledgments

366 The authors thank Editage (https://www.editage.jp) for their English language editing service. This
367 work was supported by the Japan Agency for Medical Research and Development (grant number
368 22mk0101210j0002 to Satoshi Yokota).
369

370 Conflict of interest

371 The authors do not have any conflicts of interest to declare.
372

373 Author contributions

SY conceived and designed the experiments. S Kitajima supervised this study. SY, TW, HM, KS, and MF performed the experiments. SY, TW, S Kaneko, and S Kitajima discussed the results of the data. SY drafted the manuscript. All authors critically revised the article for intellectual content.

ORCID

Satoshi Yokota: https://orcid.org/0000-0002-7660-6303

Tomohiko Wakayama: https://orcid.org/0000-0002-8795-7950

Hidenobu Miyaso: https://orcid.org/0000-0003-2212-1500

Kousuke Suga: https://orcid.org/0000-0002-4938-248X

Masakatsu Fujinoki: https://orcid.org/0000-0002-4090-160X

Satoru Kaneko: https://orcid.org/0000-0002-5249-0641

Satoshi Kitajima: https://orcid.org/0000-0002-3752-1462

387 **References**

388 1. Lanning LL, Creasy DM, Chapin RE, et al. Recommended approaches for the
389 evaluation of testicular and epididymal toxicity. *Toxicologic pathology*.
390 2002;30(4):507-520.
391 2. Scialli AR, Clark RV, Chapin RE. Predictivity of Nonclinical Male Reproductive
392 Findings for Human Effects. *Birth Defects Res*. 2018;110(1):17-26.
393 3. Rayburn ER, Gao L, Ding J, Ding H, Shao J, Li H. FDA-approved drugs that are
394 spermatotoxic in animals and the utility of animal testing for human risk prediction.
395 *J Assist Reprod Genet*. 2018;35(2):191-212.
396 4. Balhorn R. The protamine family of sperm nuclear proteins. *Genome Biol*.
397 2007;8(9):227.
398 5. Brewer LR, Corzett M, Balhorn R. Protamine-induced condensation and
399 decondensation of the same DNA molecule. *Science (New York, NY)*.
400 1999;286(5437):120-123.
401 6. Oliva R. Protamines and male infertility. *Hum Reprod Update*. 2006;12(4):417-435.
402 7. Cho C, Jung-Ha H, Willis WD, et al. Protamine 2 deficiency leads to sperm DNA
403 damage and embryo death in mice. *Biology of reproduction*. 2003;69(1):211-217.
404 8. Aoki VW, Liu L, Carrell DT. Identification and evaluation of a novel sperm
405 protamine abnormality in a population of infertile males. *Hum Reprod*.
406 2005;20(5):1298-1306.
407 9. Carrell DT, Emery BR, Hammoud S. Altered protamine expression and diminished
408 spermatogenesis: what is the link? *Hum Reprod Update*. 2007;13(3):313-327.
409 10. Cho C, Willis WD, Goulding EH, et al. Haploinsufficiency of protamine-1 or -2
410 causes infertility in mice. *Nature genetics*. 2001;28(1):82-86.
411 11. Belokopytova IA, Kostyleva EI, Tomilin AN, Vorob'ev VI. Human male infertility
412 may be due to a decrease of the protamine P2 content in sperm chromatin. *Mol Reprod*
413 *Dev*. 1993;34(1):53-57.
414 12. Kaneko S, Yoshida J, K T. Low Density Regions of DNA in Human Sperm Appear
415 as Vacuoles after
416 Translucent Staining With Reactive Blue 2. *J Med Diagn Meth*. 2013;2(6)

417 13. Xie Y, Deng CC, Ouyang B, et al. Establishing a nonlethal and efficient mouse
418 model of male gonadotoxicity by intraperitoneal busulfan injection. *Asian J Androl*.
419 2020;22(2):184-191.
420 14. Nakata H, Nakano T, Iseki S, Mizokami A. Three-Dimensional Analysis of
421 Busulfan-Induced Spermatogenesis Disorder in Mice. *Front Cell Dev Biol*.
422 2020;8:609278.
423 15. Gutierrez K, Glanzner WG, Chemeris RO, et al. Gonadotoxic effects of busulfan
424 in two strains of mice. *Reprod Toxicol*. 2016;59:31-39.
425 16. Wang DZ, Zhou XH, Yuan YL, Zheng XM. Optimal dose of busulfan for depleting
426 testicular germ cells of recipient mice before spermatogonial transplantation. *Asian*
427 *J Androl*. 2010;12(2):263-270.
428 17. Yokota S, Miyaso H, Hirai T, et al. Development of a non-invasive method for
429 testicular toxicity evaluation using a novel compact magnetic resonance imaging
430 system. *The Journal of toxicological sciences*. 2023;48(2):57-64.
431 18. Wakayama T, Yokota S, Noguchi K, Sugawara T, Sonoda K, Wanta A. Quantitative
432 evaluation of spermatogenesis by fluorescent histochemistry. *Histochem Cell Biol*.
433 2022;157(3):287-295.
434 19. Yokota S, Sekine N, Wakayama T, Oshio S. Impact of chronic vitamin A excess on
435 sperm morphogenesis in mice. *Andrology*. 2021;
436 20. Fujinoki M. Suppression of progesterone-enhanced hyperactivation in hamster
437 spermatozoa by estrogen. *Reproduction (Cambridge, England)*. 2010;140(3):453-464.
438 21. Mohri H, Inaba K, Ishijima S, Baba SA. Tubulin-dynein system in flagellar and
439 ciliary movement. *Proc Jpn Acad Ser B Phys Biol Sci*. 2012;88(8):397-415.
440 22. Hecht NB, Bower PA, Waters SH, Yelick PC, Distel RJ. Evidence for haploid
441 expression of mouse testicular genes. *Exp Cell Res*. 1986;164(1):183-190.
442 23. Hecht NB, Kleene KC, Yelick PC, Johnson PA, Pravtcheva DD, Ruddle FH.
443 Mapping of haploid expressed genes: genes for both mouse protamines are located on
444 chromosome 16. *Somat Cell Mol Genet*. 1986;12(2):203-208.
445 24. Kleene KC, Distel RJ, Hecht NB. Translational regulation and deadenylation of
446 a protamine mRNA during spermiogenesis in the mouse. *Dev Biol*. 1984;105(1):71-79.

447 25. Kleene KC. Poly(A) shortening accompanies the activation of translation of five
448 mRNAs during spermiogenesis in the mouse. *Development (Cambridge, England)*.
449 1989;106(2):367-373.
450 26. Klaus ES, Gonzalez NH, Bergmann M, et al. Murine and Human Spermatids Are
451 Characterized by Numerous, Newly Synthesized and Differentially Expressed
452 Transcription Factors and Bromodomain-Containing Proteins. *Biology of*
453 *reproduction*. 2016;95(1):4.
454 27. Gasparov VS, Degtiar VG. [Protein determination by binding with the dye
455 Coomassie brilliant blue G-250]. *Biokhimiia*. 1994;59(6):763-777. Opredelenie belka
456 po sviazyvaniiu s krasitelem kumassi brilliantovym golubym G-250.
457 28. Harms MJ, Schlessman JL, Chimenti MS, Sue GR, Damjanović A, García-Moreno
458 B. A buried lysine that titrates with a normal pKa: role of conformational flexibility
459 at the protein-water interface as a determinant of pKa values. *Protein Sci*.
460 2008;17(5):833-845.
461 29. Fitch CA, Platzer G, Okon M, Garcia-Moreno BE, McIntosh LP. Arginine: Its pKa
462 value revisited. *Protein Sci*. 2015;24(5):752-761.
463 30. Oliva R, Dixon GH. Vertebrate protamine gene evolution I. Sequence alignments
464 and gene structure. *J Mol Evol*. 1990;30(4):333-346.
465 31. Oliva R, Dixon GH. Vertebrate protamine genes and the histone-to-protamine
466 replacement reaction. *Prog Nucleic Acid Res Mol Biol*. 1991;40:25-94.
467 32. Retief JD, Winkfein RJ, Dixon GH, et al. Evolution of protamine P1 genes in
468 primates. *J Mol Evol*. 1993;37(4):426-434.
469 33. Lüke L, Vicens A, Tourmente M, Roldan ER. Evolution of protamine genes and
470 changes in sperm head phenotype in rodents. *Biology of reproduction*. 2014;90(3):67.
471 34. Miller D, Brinkworth M, Iles D. Paternal DNA packaging in spermatozoa: more
472 than the sum of its parts? DNA, histones, protamines and epigenetics. *Reproduction*
473 *(Cambridge, England)*. 2010;139(2):287-301.
474 35. Fayomi AP, Orwig KE. Spermatogonial stem cells and spermatogenesis in mice,
475 monkeys and men. *Stem Cell Res*. 2018;29:207-214.
476 36. Ward WS. Function of sperm chromatin structural elements in fertilization and
477 development. *Mol Hum Reprod*. 2010;16(1):30-36.

478 37. Ni K, Spiess AN, Schuppe HC, Steger K. The impact of sperm protamine
479 deficiency and sperm DNA damage on human male fertility: a systematic review and
480 meta-analysis. *Andrology*. 2016;4(5):789-799.
481 38. Dada R, Kumar M, Jesudasan R, Fernández JL, Gosálvez J, Agarwal A.
482 Epigenetics and its role in male infertility. *J Assist Reprod Genet*. 2012;29(3):213-223.
483 39. Bucci LR, Meistrich ML. Effects of busulfan on murine spermatogenesis:
484 cytotoxicity, sterility, sperm abnormalities, and dominant lethal mutations. *Mutat*
485 *Res*. 1987;176(2):259-268.
486 40. de Rooij DG, Kramer MF. The effect of three alkylating agents on the seminiferous
487 epithelium of rodents. I. Depletory effect. *Virchows Arch B Cell Pathol*. 1970;4(4):267-
488 275.
489 41. Rinaldi VD, Donnard E, Gellatly K, et al. An atlas of cell types in the mouse
490 epididymis and vas deferens. *Elife*. 2020;9

491

492

493 ## Figure Legends

494 **Figure 1. Distribution of reactive blue 2 (RB2)-positive male germ cells in the seminiferous**
495 **tubules.** (A, C, E, G, I, K, M, O, Q, S, U, W) Determination of stages (I–XII) and identification
496 of cell types. The nuclei of mouse control testis sections were stained with Hoechst 33258 (blue)
497 and the acrosomes were stained with PNA lectin histochemistry (green). M, spermatocytes
498 undergoing the first meiotic division; S1–16, steps 1–16 spermatids. White lines: S1–11. White
499 arrows: S12–16. Black arrows: RB2-positive S12–16 spermatids. Scale bars: 20 μm.

500

501 **Figure 2. Representative photographs of hematoxylin and eosin (HE)- or reactive blue 2**
502 **(RB2)-stained testicular cross-sections from control and busulfan-treated mice.** The incidence
503 of RB2-positive spermatids in the seminiferous tubules was examined via light microscopy. (A)
504 HE- or (D) RB2-stained sections from the testes of control mice. (B, C) HE- or (E, F) RB2-stained
505 sections from the testes of busulfan-treated mice. Black arrows: RB2-positive spermatids. (G)
506 Quantification of the percentage of RB2-positive spermatids in the seminiferous tubules from
507 control (200 tubules/section, n = 6) and busulfan-treated (200 tubules/section, n = 6) mice. Each
508 column shows the mean percentage (± SD) of seminiferous tubules not stained with RB2. Asterisks

509 indicate significant differences between the control and busulfan-treated groups (***P < 0.001).

510 Black arrows: RB2-positive spermatids. Scale bars: 20 μm.

511

512 **Figure 3. Sperm parameters in the control and busulfan-treated mice.** Percentage of (A)

513 motile or (B) hyperactivated spermatozoa in the control (n = 6) and busulfan-treated (n = 6) mice.

514 Reactive blue 2 (RB2)-stained spermatozoa from the cauda epididymis in the (C) control and (D)

515 busulfan-treated mice. RB2 staining of spermatozoa from the caput epididymis in the (E) control

516 mice and (F) busulfan-treated mice. Data are presented as mean ± SD. *P < 0.05, **P < 0.01 vs.

517 control.

518

519 **Figure 4. Representative photographs of hematoxylin (HE)- and reactive blue 2 (RB2)-**

520 **stained caput epididymal cross-sections from control and busulfan-treated mice**. Low-

521 magnification images of the morphology in the caput epididymis of (A) control and (B) busulfan-

522 treated mice. High-magnification images of the morphology in the caput epididymis of (C) control

523 and (D) busulfan-treated mice. RB2-positive spermatozoa in the caput epididymis of (E) control

524 mice adjacent to the HE-stained section (C), with no RB2 staining detected in the (F) busulfan-

525 treated group adjacent to the HE-stained section (D). (G) RB2-positive spermatozoa in the caput
526 epididymis of the control under the highest magnification (1000×). Black arrows: RB2-positive
527 spermatozoa. Scale bars: (A, B) 500 μm, (C–F) 100 μm, (G) 20 μm.
528
529 **Figure 5. Representative photographs of the mixture of reactive blue 2 (RB2) dye and**
530 **proteins.** Aggregates detected in (A, D) human protamine, (B, E) mouse synthetic protamine 1,
531 and (C, F) mouse synthetic protamine 2 standards. No aggregates were detected in the RB2 dye
532 only, bovine serum albumin standard, and intracellular proteins (without protamines) extracted
533 from HeLa cells. Scale bars: (A–C, G–I) 100 μm, (D–F) 20 μm.

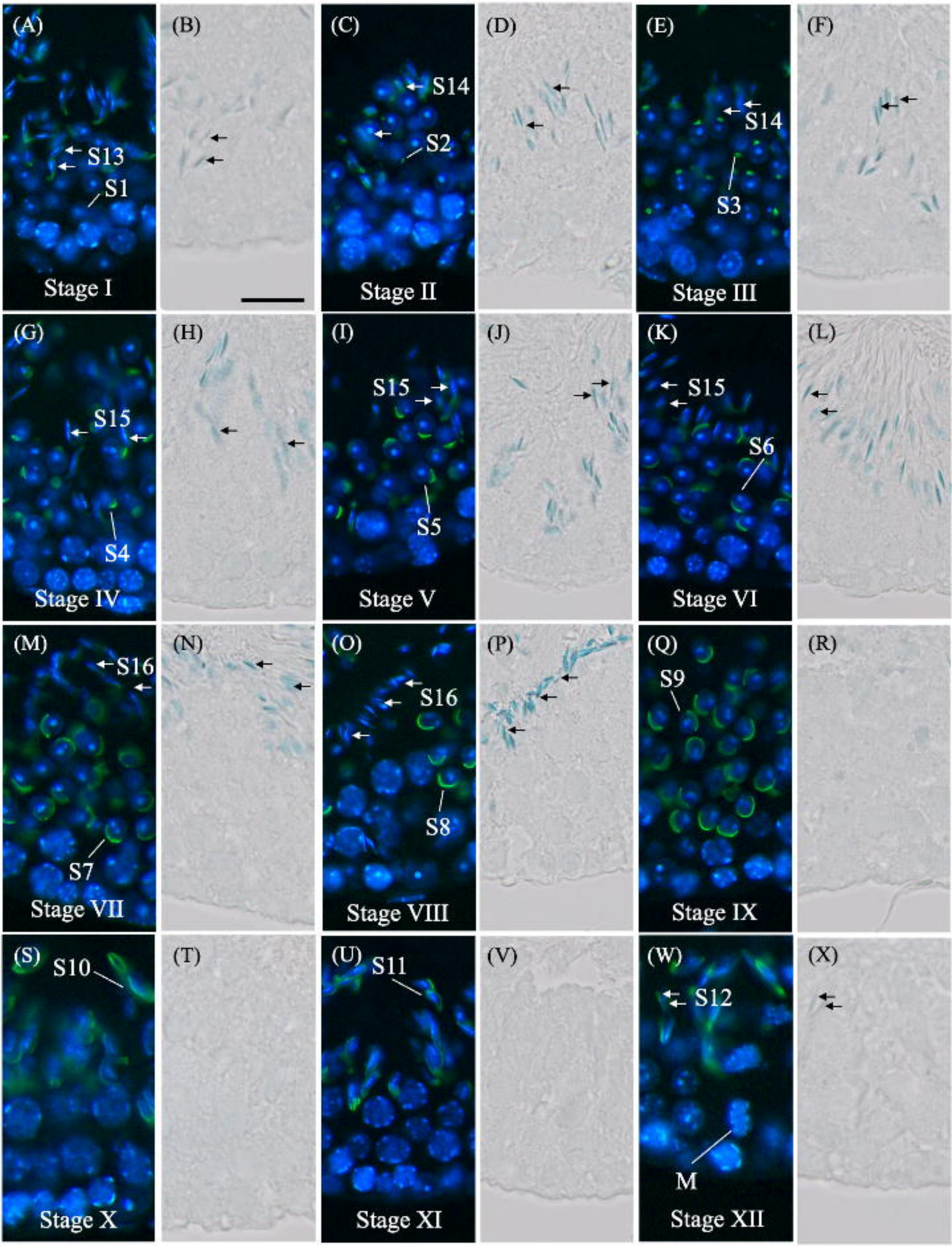
(A)
S13
S1
Stage I
(B)
(C)
S14
S2
Stage II
(D)
(E)
S14
S3
Stage III
(F)
(G)
S15
S4
Stage IV
(H)
(I)
S15
S5
Stage V
(J)
(K)
S15
S6
Stage VI
(L)
(M)
S16
S7
Stage VII
(N)
(O)
S16
S8
Stage VIII
(P)
(Q)
S9
Stage IX
(R)
(S)
S10
Stage X
(T)
(U)
S11
Stage XI
(V)
(W)
S12
M
Stage XII
(X)

Fig. 1

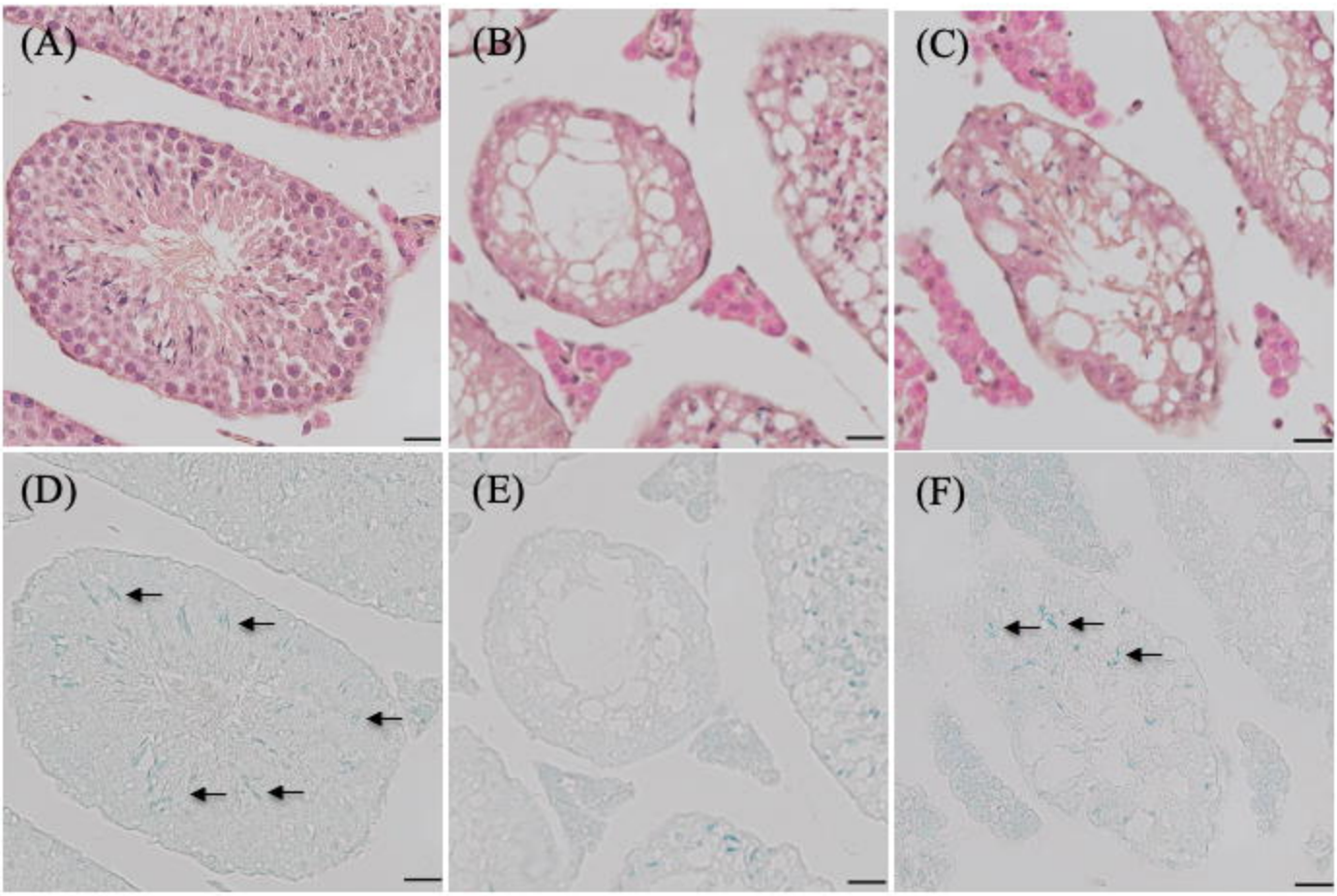
(A)
(B)
(C)
(D)
(E)
(F)

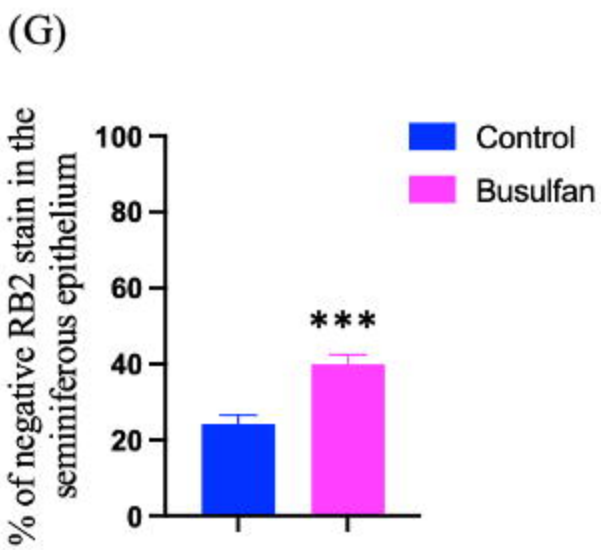
(G)
% of negative RB2 stain in the seminiferous epithelium
100
80
60
40
20
0
***
Control
Busulfan

Fig. 2

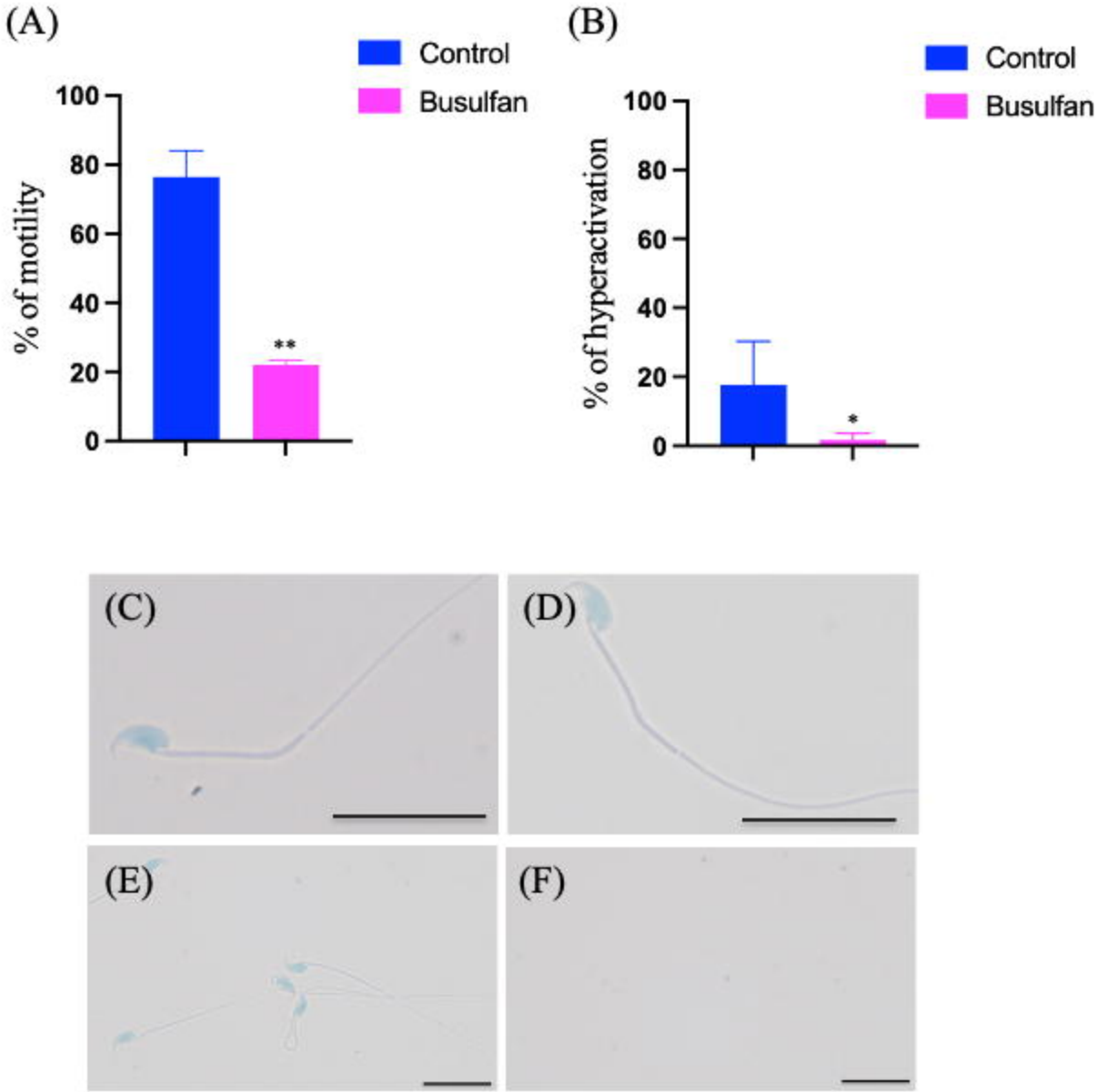
(A)
Control
Busulfan
% of motility
100
80
60
40
20
0
**
(B)
Control
Busulfan
% of hyperactivation
100
80
60
40
20
0
*
(C)
(D)
(E)
(F)

Fig. 3

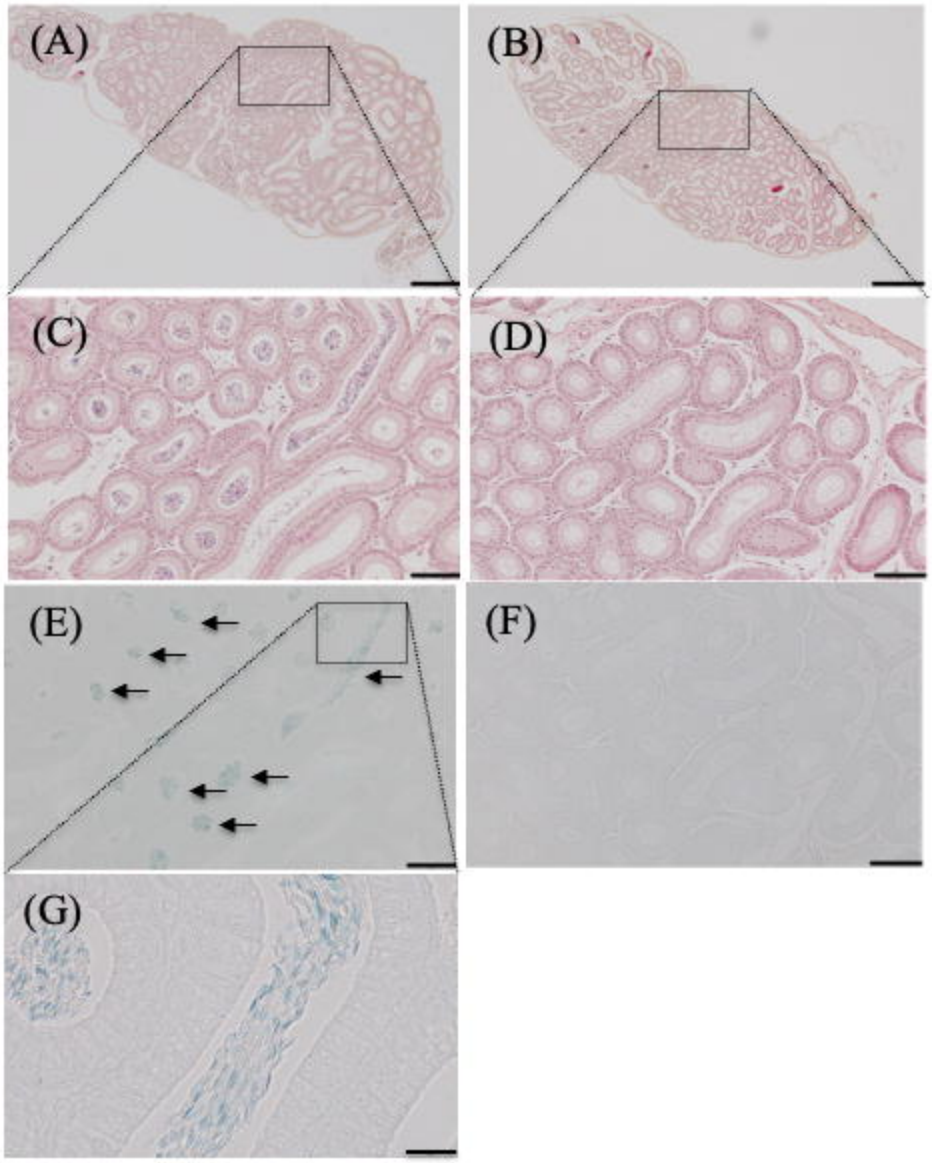

Fig. 4

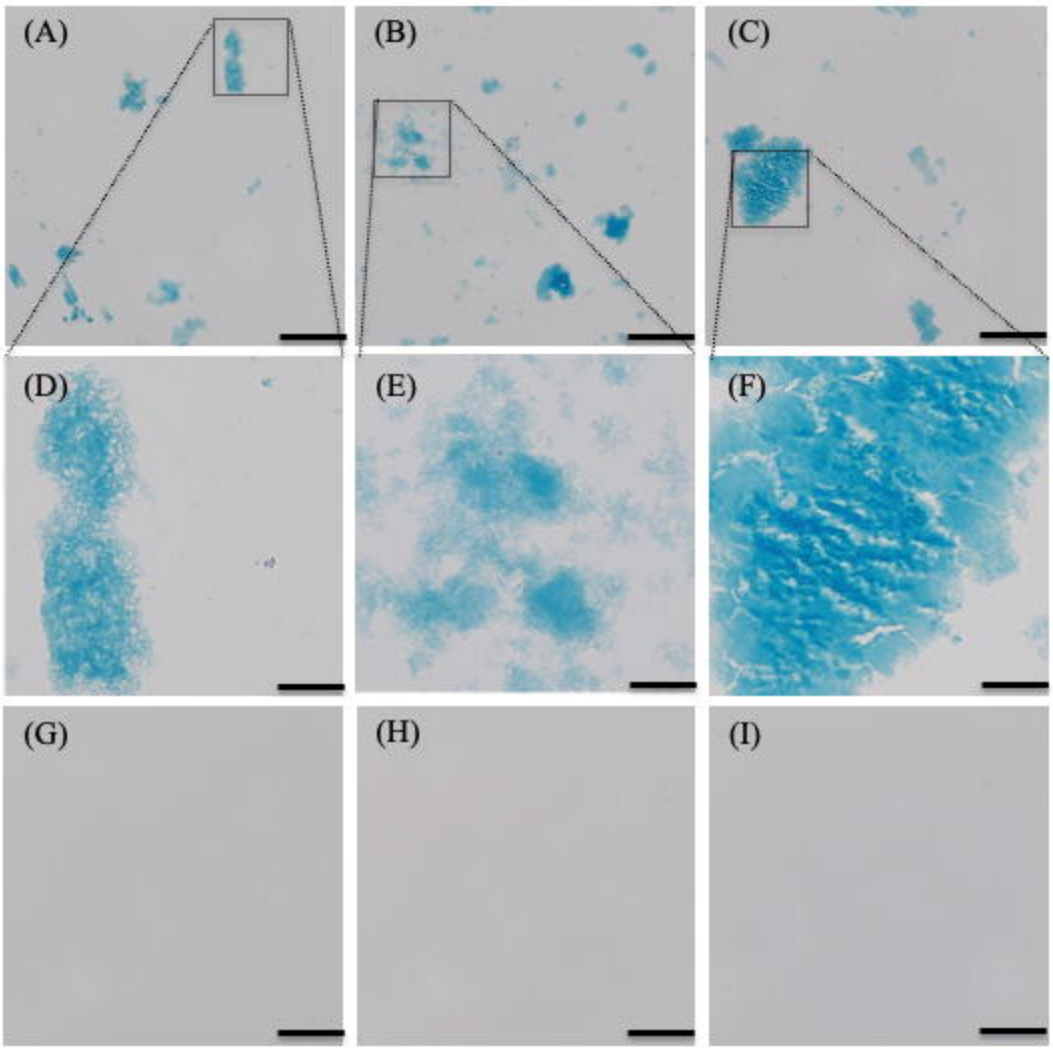

Fig. 5